Nonlinear optical line shapes of disordered molecular aggregates

Knoester, Jasper

Published in:
The Journal of Chemical Physics

DOI:
10.1063/1.465623

Publication date:
1993

Nonlinear optical line shapes of disordered molecular aggregates: Motional narrowing and the effect of intersite correlations

Jasper Knoester
Chemical Physics, Materials Science Center, University of Groningen, Nijenborgh 4, 9747 AG Groningen, The Netherlands

(Received 21 June 1993; accepted 20 August 1993)

We theoretically investigate nonlinear optical line shapes of linear molecular aggregates with Gaussian disorder in the molecular transition frequencies. A perturbative treatment in the disorder is used, within which the joint stochastic distribution function of the frequencies of *all* multiexciton states of an aggregate can be determined analytically. It is shown that motional narrowing, which is characteristic for the linear absorption spectra of aggregates, also occurs for nonlinear line shapes. An important aspect of our disorder model is that it allows for general correlations between the transition frequencies of molecules within one aggregate, thereby interpolating between continuous energy disorder and a segment or kink model. The general theory is applicable for nonlinearities of any order. Specific applications are discussed for linear absorption, nonlinear absorption, and two-color pump–probe spectra. Our theory suggests that pump–probe experiments provide a novel and very promising approach to obtain microscopic information on aggregate systems; in particular, this technique can be used to determine both the magnitude of the molecular disorder and its degree of intersite correlation within aggregates.

I. INTRODUCTION

Even though the spectroscopy of molecular J aggregates has been studied for more than five decades already,[1] there continues to be a strong interest in the optical properties of these systems.[2] The most characteristic property of J aggregates is the fact that their absorption spectra exhibit a sharp feature (the J band) that is typically much narrower than the absorption bands observed in monomer spectra. The sharpness results from motional narrowing—the delocalized exciton states of the aggregate average over the disorder in the transition frequencies of the individual molecules. The term "motional narrowing" was first introduced in the field of nuclear magnetic resonance, where it refers to the narrowing of inhomogeneous line shapes due to rotational motion of the spins.[3] The simplest quantitative explanation for motional narrowing in the *linear* absorption spectrum of J aggregates can be given by considering the probability distribution of each of the exciton energies to first order in the molecular disorder.[4] If the molecular transition frequencies on each aggregate are distributed completely uncorrelated of each other, this procedure predicts a narrowing of the local (molecular) disorder by a factor of typically $1/\sqrt{N}$ (N being the number of molecules per aggregate). Recently, also the *nonlinear* optical properties of J aggregates have received a growing attention. On the one hand, time-resolved nonlinear techniques are used to probe dynamic features of the exciton system[5,6] and transitions to multiexciton states,[7,8] in which the molecules on the aggregate share more than one excitation. On the other hand, the cw nonlinear optical response is of interest,[9,10] as the giant oscillator strengths of the delocalized states in principle allow for large nonlinear optical signals.[11–14] Although numerical simulations have shown that also in nonlinear optical spectra of aggregates motional narrowing takes place,[15,16] a systematic theory treating this problem is still lacking. The problem is more complicated than for linear spectroscopies because nonlinear techniques usually involve more than one (multi)exciton level of the aggregates.[2,15,16] Therefore, the motional narrowing theory of nonlinear optics requires knowledge of the joint probability distribution for the energies of two or more multiexciton states of an aggregate.

In the present paper, we investigate the motional narrowing theory of nonlinear optical response for linear molecular aggregates with diagonal disorder with *arbitrary degree of correlation* between the random transition frequencies of the molecules within each aggregate. Even though in realistic systems intersite correlations in the disorder are very likely, their extent is usually unknown and they are mostly neglected in model calculations. The model assumed in this paper interpolates between two opposite views of disorder in aggregates and polymers:[17] (i) continuous energy disorder, where the transition frequencies of the molecules within each aggregate are completely uncorrelated; and (ii) a segment (or kink) model, where all molecules within an aggregate have the same transition frequency, whose value varies for different aggregates.[18] It turns out that for the general model presented here, we can calculate the *complete multivariate probability distribution of all (multi)exciton energies* of an aggregate to first order in the disorder. Our aim to put this result to use is twofold. First, knowledge of this distribution allows us to extend the usual theory of motional narrowing to nonlinear optical line shapes of arbitrary order. Second, we investigate what optical experiments enable us to obtain information on the two parameters that determine the microscopic disorder model—the local inhomogeneity and the degree of correlation. The effect of correlations has earlier been studied by Knapp for circular aggregates within the context of linear optics.[4] It turns out, however, that measurement of the linear absorption line shape is not a very good tool to

 0021-9606/93/99(11)/8466/14/$6.00

decide what microscopic disorder model applies to a certain sample (see Sec. V A). By contrast, we will show that nonlinear techniques, such as pump–probe experiments, can provide much more insight.

We note that the situation outlined above (continuous energy disorder vs a segment model) is reminiscent of the question of microscopic vs macroscopic strain broadening in (mixed) crystals. Photon echo experiments have been suggested to distinguish been these two cases.[19,20] Root and Skinner even considered an interpolation between these two limits by considering a crystal model with a finite correlation length of the strain field.[21] The theory in the present paper is more specifically directed toward molecular aggregates and, moreover, is directly applicable to any nonlinear optical experiment.

The outline of this paper is as follows: in Sec. II, we present the microscopic model of disordered aggregates and define the motional narrowing approximation for their eigenstates and eigenenergies. In Sec. III, we show how the distribution of exciton energies enters the nonlinear optical response of an ensemble of disordered aggregates. The complete joint distribution function for the (multi)exciton levels in such an ensemble is obtained in Sec. IV. This distribution is used in Sec. V to calculate explicitly the line shapes for linear absorption, nonlinear absorption, and two-color pump–probe spectroscopy within the motional narrowing limit. Finally, in Sec. VI, we discuss our results. Two appendices are added for technical details.

II. MODEL AND EIGENSTATES

We consider an ensemble of molecular aggregates with energetic disorder. Each aggregate consists of a linear chain of N equidistant nonpolar two-level absorbers with parallel transition dipoles of magnitude μ. We stress that *no* periodic boundary conditions are assumed. The electronic states of an aggregate are described by the Frenkel exciton Hamiltonian[22,23]

$$\hat{H}_0=\hbar\sum_{n=1}^{N}(\omega_0+d_n)\hat{B}_n^{\dagger}\hat{B}_n+\hbar\sum_{n=1}^{N-1}V(\hat{B}_n^{\dagger}\hat{B}_{n+1}+\hat{B}_{n+1}^{\dagger}\hat{B}_n)$$
$$\equiv\hbar\sum_{n,m}H_{nm}\hat{B}_n^{\dagger}\hat{B}_m. \tag{1}$$

Here $\hat{B}_n$ and $\hat{B}_n^{\dagger}$ denote the Pauli annihilation and creation operators for an excitation on molecule n, respectively, and ω_0+d_n is the transition frequency of molecule n, where ω_0 is the average transition frequency and d_n is a static random offset which describes diagonal disorder. Finally, V is the nearest-neighbor interaction, which is negative for J aggregates. V is assumed to be homogeneous; interactions between different aggregates are neglected.

Following Knapp,[4] we assume that the molecular frequency offsets of a single aggregate have the following Gaussian joint distribution:

$$\bar{P}^{(N)}(d_1,\ldots,d_N)=\frac{1}{(2\pi)^{N/2}\sqrt{\det A}}\times\exp\left(-\frac{1}{2}\sum_{n,m=1}^{N}A_{nm}^{-1}d_nd_m\right), \tag{2}$$

where A_{nm}^{-1} denotes the nmth element of the inverse of the covariance matrix A. For A, we take the positive definite matrix

$$A_{nm}\equiv\langle d_nd_m\rangle=a_0^2\exp(-|n-m|/l_0). \tag{3}$$

Here, a_0 gives the magnitude of the molecular disorder and l_0 is the correlation length of the disorder in units of the lattice constant. Note that a_0 equals the standard deviation of the Gaussian marginal distribution[24] for the frequency offset of a single molecule regardless of the values of the other frequencies

$$\bar{P}^{(1)}(d_n)\equiv\int\bar{P}^{(N)}(d_1,\ldots,d_N)dd_1\cdots dd_{n-1}dd_{n+1}\cdots dd_N$$
$$=\frac{1}{\sqrt{2\pi}a_0}\exp(-d_n^2/2a_0^2). \tag{4}$$

The present disorder model interpolates continuously between completely uncorrelated inhomogeneities for $l_0\to0$ and infinitely strong correlations for $l_0\to\infty$. The former limit is known as the continuous energy disorder model and the latter as a segment model.[17] In the segment model, all molecules on a given aggregate have the same transition frequency, which is chosen randomly from a Gaussian with standard deviation a_0.[18]

To determine the nonlinear optical response of an ensemble of noninteracting disordered aggregates through standard response theory (sum over states procedure),[25,26] we have to calculate the eigenstates of a molecular chain with arbitrary realization of the disorder. Because $\hat{H}_0$ conserves the number of excitations, the eigenstates separate into classes of linear combinations of states with a fixed number of molecules excited—exciton bands (Fig. 1). Using the Jordan–Wigner transformation[27] from the interacting Paulions to noninteracting Fermions, all 2^N eigenstates of $\hat{H}_0$ can be obtained by only diagonalizing the tridiagonal $N\times N$ matrix H_{nm}, irrespective of the disorder.[15,28] Let the normalized eigenvectors of $\hat{H}_0$ (for a particular realization of the disorder) have components φ_{kn} and eigenvalues Ω_k ($k=1,\ldots,N$). Then a general eigenstate in the νth band may be labeled by $k_1>k_2>\cdots>k_\nu$ and reads

$$|k_1,k_2,\ldots,k_\nu\rangle=\sum_{n_\nu>\cdots>n_2>n_1}\det(\varphi_{k_1n_1},\varphi_{k_2n_2},\ldots,\varphi_{k_\nu n_\nu})\times|n_1,n_2,\ldots,n_\nu\rangle, \tag{5a}$$

where $|n_1,n_2,\ldots,n_\nu\rangle$ denotes the state with sites $n_1,n_2,\ldots,n_\nu$ excited and the remainder in the ground state and $\det(\cdots)$ denotes the Slater determinant of the φ_{kn} components. The frequency of this state is given by

$$\Omega_{k_1k_2\cdots k_\nu}=\Omega_{k_1}+\Omega_{k_2}+\cdots+\Omega_{k_\nu}. \tag{5b}$$

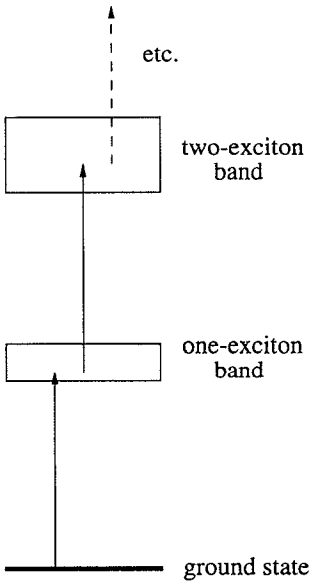

FIG. 1. A schematic representation of the lower part of the energy level scheme of an aggregate of two-level molecules. The excited states occur in exciton bands, in which the total number of excitations shared by the molecules is a constant. The separation between consecutive bands is of the order of the average molecular transition frequency, whereas the width of the n-exciton band is of the order of $4n$ times the intermolecular interaction. Optical transitions are only allowed between adjacent bands.

Thus the one-excitons (conventional Frenkel excitons) have site amplitudes φ_{kn} and frequencies Ω_k; the states in higher exciton bands (two-excitons, three-excitons, etc.) have energies that are given by a sum of one-exciton energies, whereas their coefficients in the site basis are generated by Slater determinants of the one-exciton site amplitudes. The simplicity of the representation of these states and their energies is special for the linear system with nearest-neighbor interactions. Two points should be stressed concerning the multiexciton states. (i) They are *not* direct products of one-exciton states, as is clear from Eq. (5a); this is a consequence of the Pauli exclusion principle—a molecule cannot be doubly excited. (ii) They are unbound (continuum) states; in particular, the two-excitons referred to here should not be confused with biexciton states, which represent a bound pair of excitations.[23] We finally note that optical transitions can only occur between two adjacent exciton bands.

In spite of the enormous simplification of the calculation of the eigenstates through the Jordan–Wigner transformation, the diagonalization of H_{nm} and the final disorder average in general involve numerical procedures. Only for homogeneous aggregates ($a_0=0$) is it possible to diagonalize H_{nm} analytically. We then have

$$\varphi^0_{kn}=\sqrt{\frac{2}{N+1}}\sin\left(\frac{\pi kn}{N+1}\right) \tag{6a}$$

and

$$\Omega^0_k=\omega_0+2V\cos\left(\frac{\pi k}{N+1}\right), \tag{6b}$$

where the superscript 0 is used to indicate quantities pertinent to the homogeneous system. The eigenvectors φ^0_{kn} are standing waves which are delocalized over the entire chain. For small values of the disorder (a_0), we may now resort to an expansion around the homogeneous system, the perturbation being

$$\hat{H}_{\rm pert}=\hbar\sum_{n=1}^{N} d_n\hat{B}_n^\dagger\hat{B}_n. \tag{7}$$

The smallness parameter for this expansion is $a_0N^{3/2}/\pi^2|V|$ (see Ref. 4 and Sec. VI). In a lowest-order treatment, we will use the eigenfrequencies to first order in $\hat{H}_{\rm pert}$ and the unperturbed eigenstates, which implies that the transition dipoles between the exciton states are taken identical to those for the homogeneous aggregate. Because this approach, known as the motional narrowing limit, has provided much insight into the linear absorption spectra of J aggregates,[4] we will use it in this paper to analyze the general *nonlinear* response of disordered aggregates. The motional narrowing limit has previously been used to calculate the photon echo decay of circular aggregates with uncorrelated disorder.[29]

III. NONLINEAR OPTICAL RESPONSE IN THE MOTIONAL NARROWING LIMIT

The nonlinear optical response of a single aggregate with a specific realization of the diagonal disorder can be represented by its (hyper)polarizabilities, which are fully determined by the frequencies and transition dipoles of the multiexciton states. Let the nth order polarizability be denoted $\gamma^{(n)}(\omega;\Omega)$, where ω is a $(n+1)$-dimensional vector containing the laser frequencies and the signal frequency that occur in the process. The dependence on the exciton energies is denoted explicitly by the argument $\Omega\equiv(\Omega_1,\ldots,\Omega_N)$. We reiterate that for the linear chain, these N eigenfrequencies of H_{nm} determine not only the N one-exciton frequencies, but also *all* the multiexciton frequencies. In the above notation, we omitted the dependence of the polarizability on the transition moments between the various multiexciton states because, within the motional narrowing limit, these do not depend on the particular realization of the disorder. The nth order macroscopic susceptibility of a sample containing a random distribution of noninteracting aggregates may then be written

$$\chi^{(n)}(\omega)=\eta\langle\gamma^{(n)}(\omega;\Omega)\rangle. \tag{8}$$

Here, η is the density of aggregates in the sample and $\langle\cdots\rangle$ denotes the average over the diagonal disorder, i.e., over the probability distribution [Eq. (2)]. In writing Eq. (8), we have assumed that all aggregates have equal orientation, so that the transition dipoles for all aggregates are parallel. A more general distribution of aggregate orientations can be accounted for in a straightforward way by an angular factor[16] and does not affect the diagonal disorder average and the spectral line shapes derived from $\chi^{(n)}$. Equation (8) may be rewritten

$$\chi^{(n)}(\omega)=\eta\int\gamma^{(n)}(\omega;\Omega^0+\mathbf{D})P^{(N)}(\mathbf{D})dD_1\cdots dD_N. \tag{9}$$

Here, $D_k\equiv\Omega_k-\Omega_k^0$, the deviation of the kth eigenfrequency of H_{nm} from its homogeneous value to first order in the disorder and $P^{(N)}(D_1,...,D_N)$ is the joint probability distribution for these deviations to occur on a randomly generated aggregate. Hereafter, we will refer to $P^{(N)}(D_1,...,D_N)$ as the distribution for the exciton frequencies. In Sec. IV, we will derive this distribution from the underlying molecular disorder distribution $\bar{P}^{(N)}(d_1,...,d_N)$. There are two advantages to working with the distribution for the exciton frequencies. (i) The hyperpolarizabilities depend directly on the exciton frequencies and only in an indirect way on the molecular frequencies. (ii) The hyperpolarizabilities of low order consist of additive contributions containing only a small number of exciton frequencies. Therefore, only marginal distributions[24] for small subsets of $(D_1,...,D_N)$ are needed in practice and the disorder average [Eq. (9)] only involves a small number of integrations. The simplest case is the linear susceptibility, for which it suffices to know the marginal distribution for a single one-exciton frequency (see Sec. V A).

IV. JOINT PROBABILITY DISTRIBUTION FOR THE EXCITON FREQUENCIES

In this section, we calculate the complete multivariate distribution of the exciton frequencies to first order in the disorder Hamiltonian (7). For a particular realization of the disorder, we have

$$D_k={}^0\langle k|\hat{H}_{\rm pert}|k\rangle^0=\sum_{n=1}^{N}|\varphi_{kn}^0|^2d_n, \tag{10}$$

with φ_{kn}^0 given by Eq. (6a). From Eq. (10), we observe that every D_k is a linear combination of the Gaussian variables d_n. Consequently, also the D_k have a Gaussian joint distribution, which, as $\langle D_k\rangle=0$ for all k, is fully determined by its covariance matrix

$$B_{kk'}\equiv\langle D_kD_{k'}\rangle=\sum_{n,m=1}^{N}|\varphi_{kn}^0\varphi_{k'm}^0|^2A_{nm}, \tag{11}$$

with A_{nm} as defined in Eq. (3). In Appendix A, the double summation in this equation is performed and we arrive at

$$B_{kk'}=\left(\frac{a_0}{N+1}\right)^2\Bigg\{(N+1)\frac{1+\beta}{1-\beta}-2(1-\beta^{N+1})f(k)f(k')+\frac{1}{4}(N+1)(1-\beta^2)\left[\frac{1}{g(k)}+\frac{1}{g(k')}\right]\times(\delta_{k,k'}+\delta_{k+k',N+1})\Bigg\}, \tag{12}$$

where

$$f(k)=\frac{1}{1-\beta}-\frac{1-\beta\cos[2\pi k/(N+1)]}{1-2\beta\cos[2\pi k/(N+1)]+\beta^2}, \tag{13a}$$

$$g(k)=1-2\beta\cos[2\pi k/(N+1)]+\beta^2. \tag{13b}$$

Above, we have introduced the parameter

$$\beta\equiv\exp(-1/l_0)=\langle d_nd_{n+1}\rangle/\langle d_n^2\rangle, \tag{14}$$

which gives the degree of correlation between the transition frequencies of the molecules within one chain. For $\beta=0$ ($l_0=0$), all molecular frequencies are chosen independently of each other from $\bar{P}^{(1)}(d_n)$ given in Eq. (4); for $\beta=1$ ($l_0\to\infty$), we have the case of infinitely strong correlations.

The general joint distribution for the D_k is now given by

$$P^{(N)}(D_1,...,D_N)=\frac{1}{(2\pi)^{N/2}\sqrt{\det B}}\times\exp\left(-\frac{1}{2}\sum_{k,k'=1}^{N}B_{kk'}^{-1}D_kD_{k'}\right). \tag{15}$$

Of course, $B_{kk'}$ may alternatively be used to describe the marginal distribution for any subset $\{D_{k_1},...,D_{k_s}\}$ ($s<N$). This distribution is also Gaussian with vanishing means and is fully determined by the $s\times s$ covariance matrix $B_{kk'}(k,k'\in\{k_1,...,k_s\})$. The simplest marginal distribution is the one for a single one-exciton frequency D_k,

$$P^{(1)}(D_k)=\exp(-D_k^2/2\sigma_k^2)/\sqrt{2\pi}\sigma_k, \tag{16a}$$

with the variance $\sigma_k^2=B_{kk}$. More complicated examples are the joint probability distributions for two or more one-exciton levels, e.g., $P^{(2)}(D_k,D_{k'})$ ($k\neq k'$),

$$P^{(2)}(D_k,D_{k'})=\frac{1}{2\pi\sqrt{B_{kk}B_{k'k'}-B_{kk'}^2}}\times\exp\left(-\frac{1}{2}\frac{B_{k'k'}D_k^2+B_{kk}D_{k'}^2-2B_{kk'}D_kD_{k'}}{B_{kk}B_{k'k'}-B_{kk'}^2}\right), \tag{16b}$$

which does not reduce to $P^{(1)}(D_k)P^{(1)}(D_{k'})$ because $B_{kk'}\neq0$ in general. Yet other examples of subset distributions are those for the value of a multiexciton frequency. It is easily seen that the deviation of the energy of the multiexciton $|k_1,...,k_\nu\rangle$ from its homogeneous value $\Omega_{k_1}^0+\Omega_{k_2}^0+\cdots+\Omega_{k_\nu}^0$ has a Gaussian distribution with zero mean and variance

$$\sigma_{k_1\cdots k_\nu}^2=\sum_{i,j=1}^{\nu}B_{k_ik_j}. \tag{17}$$

It is also possible to compose the joint probability distributions for a few (multi)exciton levels in this manner.

Before applying the above probability distributions to special spectroscopic techniques (Sec. V), we point out that degeneracies occur in $P^{(N)}(D_1,...,D_N)$, independent of a_0 and β. That this should be the case becomes clear from combining Eqs. (6a) and (10)

$$D_k=\frac{1}{N+1}\sum_{n=1}^{N}\{1-\cos[2\pi k/(N+1)]\}d_n, \qquad (18)$$

which shows that $D_{N+1-k}=D_k$ independent of the probability distribution of the d_n. This degeneracy is also seen explicitly in the covariance matrix B. According to Eq. (12), we have $B_{kk'}=B_{k,N+1-k'}$. Thus, B has a large number ($N/2$ for N even) of pairs of columns that are equal, yielding $\det B=0$, so that $P^{(N)}$ in Eq. (15) seems ill defined. Of course, this is just a manifestation of the fact that in some directions of the N-dimensional frequency space, $P^{(N)}$ has a vanishing width and a delta-function character. For even N, this may be made more explicit by writing

$$P^{(N)}(D_1,\ldots,D_N)$$

$$=P^{(N/2)}(D_1,\ldots,D_{N/2})\prod_{k=N/2+1}^{N}\delta(D_k-D_{N+1-k}), \qquad (19)$$

where $P^{(N/2)}(D_1,\ldots,D_{N/2})$ is the $N/2$-dimensional Gaussian distribution with vanishing means and covariance matrix $B_{kk'}(k,k'\in\{1,\ldots,N/2\})$. If N is odd, Eq. (19) is modified in a trivial way by realizing that $D_{(N+1)/2}$ is not paired to any other one-exciton frequency.

To conclude this section, we note an important difference between linear and circular aggregates. In the latter case, one imposes periodic boundary conditions on each aggregate, by adding the term $V(\hat{B}_N^{\dagger}\hat{B}_1+\hat{B}_1^{\dagger}\hat{B}_N)$ to the Hamiltonian equation (1). Then the homogeneous one-exciton site amplitudes are given by $\tilde{\varphi}_{kn}^0=\exp(-2\times\pi ikn/N)/\sqrt{N}$ $(k=0,1,\ldots,N-1)$, so that $D_k=\Sigma_n d_n/N$ [cf. Eq. (10)], which is independent of k. To first order in the disorder, all one-exciton frequencies for the circular aggregate are shifted by the same amount, irrespective of the degree of intersite correlation. Even though the Jordan–Wigner transformation does not bring the Hamiltonian with periodic boundary conditions into a free-Fermion form,[28] the structure of the *homogeneous* multiexciton states for circular aggregates is known[30] and it can be shown that to first order in the disorder, every state in the νth band is shifted by $\nu\Sigma_n d_n/N$, again independent of the degree of correlation. Many aggregate properties do not depend sensitively on whether one considers periodic boundary conditions or not; the (unphysical) infinitely strong correlations of the exciton frequencies noted here constitute a counterexample, which is important for *non*linear line shapes. Of course, in the limit $N\to\infty$, the choice of boundary conditions should become irrelevant, but that limit lies outside the motional narrowing regime, as the perturbation theory breaks down for large N. Another well-known limitation of the circular model is that for fixed nearest-neighbor interaction, the frequency of the band edge state does not depend on the aggregate size. This becomes essential if a segment length distribution determines the width of the exciton absorption line.[31]

V. APPLICATION TO OPTICAL LINE SHAPES

A. Linear absorption line shape

Although the motional narrowing theory of the linear absorption spectrum has been treated in depth by Knapp,[4] we will briefly revisit this basic example and discuss the possibility to determine microscopic parameters from observed line shapes. The linear absorption line shape is given by $A_{\rm lin}(\omega)=\mathrm{Im}\,\chi^{(1)}(\omega;\boldsymbol{\Omega})=\eta\langle\mathrm{Im}\,\gamma^{(1)}(\omega;\boldsymbol{\Omega})\rangle$, where $\boldsymbol{\omega}$ stands for $(-\omega,\omega)$. Within the motional narrowing limit and in the rotating wave approximation (RWA), the linear polarizability of a single aggregate, which in the absence of fields is in its ground state, is given by[16,26]

$$\gamma^{(1)}(\omega;\boldsymbol{\Omega}^0+\mathbf{D})=-\frac{1}{\hbar}\sum_{k=1}^{N}\frac{\mu_{0k}\mu_{k0}}{\omega-\Omega_k^0-D_k+i\Gamma}, \qquad (20)$$

where μ_{0k} is the transition dipole matrix element between the ground state and the homogeneous one-exciton $|k\rangle$, and Γ is the damping rate of the coherence between the ground state and a one-exciton state (for simplicity assumed independent of k). As Eq. (20) is a sum of contributions from individual one-exciton states, the disorder average only involves the marginal distribution $P^{(1)}(D_k)$ given in Eq. (16a). From Eq. (12), it is found that the width $\sigma_k=\sqrt{B_{kk}}$ of this Gaussian distribution varies from $a_0[2(N+1)/3]^{-1/2}$ for $\beta=0$ to a_0 for $\beta\to 1$. Both limits are independent of k {except for the case $k=(N+1)/2$, where the $\beta=0$ width is replaced by $a_0[(N+1)/2]^{-1/2}$}, but the full β dependence of the width does depend slightly on k. As long as $1-\beta\gg\beta[2\pi k/(N+1)]^2$, the β dependence simplifies to

$$\sigma_k\approx\sqrt{\frac{1+\beta}{1-\beta}}\,a_0\left[\frac{3}{2(N+1)}\right]^{1/2} \qquad (21)$$

$[k\neq(N+1)/2]$. The factor $[(1+\beta)/(1-\beta)]^{1/2}$ has also been found by Knapp[4] for circular aggregates in the limit $\beta^N\ll 1$, i.e., for large aggregates and β sufficiently different from unity. These conditions are similar to the ones under which Eq. (21) is valid.

In general, the disorder average of Eq. (20) leads to a series of N Voigt profiles[32] centered around the homogeneous one-exciton frequencies Ω_k^0. We will assume, however, that the homogeneous width $\Gamma\ll a_0[2(N+1)/3]^{-1/2}$. In that case, we have

$$A_{\rm lin}(\omega)=\frac{\pi\eta}{\hbar}\sum_{k=1}^{N}|\mu_{0k}|^2P^{(1)}(\omega-\Omega_k^0), \qquad (22)$$

which is a series of N Gaussian peaks with widths σ_k and weights the one-exciton oscillator strengths given by

$$|\mu_{0k}|^2=\left(\sum_{n=1}^{N}\mu\varphi_{kn}^0\right)^2$$

$$=\mu^2\frac{2}{N+1}\frac{[1-(-1)^k]^2}{4}\cot^2\left[\frac{\pi k}{2(N+1)}\right]. \qquad (23)$$

As almost the entire oscillator strength $[0.81(N+1)\mu^2$ for

$N \gg 1$] between the ground state and the one-exciton band resides in the $|k=1\rangle$ one-exciton state, the linear absorption spectrum is, within the motional narrowing limit, dominated by a Gaussian peak (the "*J*-band") positioned at $\Omega^0_{k=1}$ with a width $\sigma_{k=1}$ (in the remainder of this paper, we will reserve the word "width" for the standard deviation of the line shape; for Gaussian profiles, this width is smaller than the full width at half-maximum (FWHM) by a factor of $(8 \ln 2)^{1/2} \approx 2.35$). Thus, in the absence of correlations ($\beta=0$), the linear absorption spectrum has a width of $a_0[2(N+1)/3]^{-1/2}$, which explains the characteristic narrowing of the local disorder a_0 observed for *J* aggregates.[1] (For circular aggregates, one finds a width of $a_0/\sqrt{N}$.[4]) The physical explanation for this motional narrowing is that the delocalized exciton states average over the N uncorrelated molecular transition frequencies in the aggregate. In the case of perfect correlations ($\beta=1$), each individual aggregate is homogeneous, so that no averaging of local inhomogeneities occurs and the narrowing disappears. The full β dependence of the width of the *J* band is given in Fig. 2 for several aggregate sizes.

Suppose now that the typical number of molecules within an aggregate is known (for instance, from the ratio of the superradiant and the single molecule spontaneous emission rates[5(a),5(b),33,34]). Then the above shows that to explain an observed width of the *J* band, one arrives at two different values of a_0, which differ by a factor of roughly $\sqrt{N}$, depending on whether one assumes perfect correlations or total absence of correlations. More generally formulated, even if N is known, the width of the linear absorption spectrum does not yield sufficient information to determine uniquely the microscopic disorder model, as both a_0 and β are unknown. Conversely, Eq. (21) has been used to obtain N from measurement of the width of the linear absorption spectrum by assuming that a_0 can be taken from the monomer absorption spectrum.[5(a)] Here too, one lacks uniqueness, as the degree of correlation β is unknown. Moreover, the assumption that the width of a dilute distribution of monomers can be used as local inhomogeneity in dense, aggregate forming solutions (or glasses) seems highly questionable. These problems call for alternative spectroscopic techniques to characterize the microscopic disorder model.

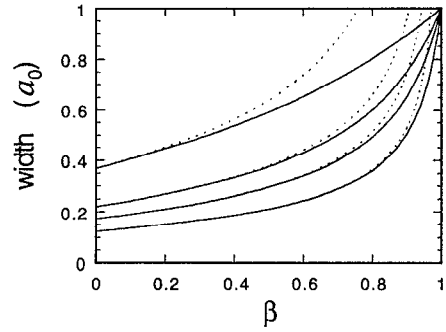

FIG. 2. Width $\sigma_{k=1}=\sqrt{B_{11}}$ *of the J* band in the motional narrowing limit as a function of the degree of intersite correlation β. Solid lines give the exact result, derived from Eq. (12); the dotted lines correspond to the small-β approximation (21). From top to bottom, the curves correspond to aggregates of $N=10$, 30, 50, and 100 molecules, respectively.

B. Nonlinear absorption spectrum

The nonlinear absorption coefficient of a cw laser beam is to lowest order in the intensity governed by $A_{\rm nl}(\omega) = \mathrm{Im}\,\chi^{(3)}(\omega;\mathbf{\Omega}) = \eta\langle \mathrm{Im}\,\gamma^{(3)}(\omega;\mathbf{\Omega})\rangle$, where ω now stands for $(-\omega,\omega,\omega,-\omega)$, and $\mathbf{\Omega}$ denotes, as before, the set of N frequencies Ω_k. The general expression for the third-order polarizability of an aggregate has been derived before.[2,12(b),16] In the RWA and within the motional narrowing limit, we have for the component needed here

$$\gamma^{(3)}(\omega;\mathbf{\Omega}^0+\mathbf{D}) = \gamma^{(3)}_{\rm bl}(\omega;\mathbf{\Omega}^0+\mathbf{D}) + \gamma^{(3)}_{\rm TPA}(\omega;\mathbf{\Omega}^0+\mathbf{D}) \tag{24a}$$

with

$$\gamma^{(3)}_{\rm bl}(\omega;\mathbf{\Omega}^0+\mathbf{D}) = \frac{2}{8\hbar^3}\sum_{k_1,k_2=1}^{N} \frac{|\mu_{0k_1}\mu_{0k_2}|^2}{(\Delta_{k_1}+i\Gamma)(\Delta_{k_2}-i\Gamma)}\left(\frac{1}{\Delta_{k_1}+i\Gamma}+\frac{1}{\Delta_{k_2}+i\Gamma}\right), \tag{24b}$$

$$\gamma^{(3)}_{\rm TPA}(\omega;\mathbf{\Omega}^0+\mathbf{D}) = -\frac{4}{8\hbar^3}\sum_{\substack{k_1,k_2,k_3,k_4=1\\(k_3>k_4)}}^{N} \frac{\mu_{0k_2}\mu_{k_2,k_3k_4}\mu_{k_3k_4,k_1}\mu_{k_10}\Delta_{k_2}}{(\Delta^2_{k_2}+\Gamma^2)(\Delta_{k_1}+i\Gamma)(\Delta_{k_3}+\Delta_{k_4}+2i\Gamma)}. \tag{24c}$$

Here, $\Delta_k \equiv \omega-\Omega^0_k-D_k$ and μ_{k,k_1k_2} denotes the transition dipole matrix element between the homogeneous one-exciton $|k\rangle$ and two-exciton $|k_1,k_2\rangle$, for which a general expression can be found in Ref. 16. The first contribution ($\gamma^{(3)}_{\rm bl}$) only involves one-excitons as intermediate states in the nonlinear process; as long as Γ is small compared to the separation between two one-exciton states, its main signature in the nonlinear absorption spectrum is a bleach of the one-exciton transitions

$$A_{\rm nl,bl}(\omega) = -\left\langle \frac{\eta\Gamma}{2\hbar^3}\sum_{k=1}^{N} \frac{|\mu_{0k}|^4}{[(\omega-\Omega^0_k-D_k)^2+\Gamma^2]^2}\right\rangle. \tag{25}$$

As for the linear absorption spectrum, the disorder average in Eq. (25) only involves the marginal distribution $P^{(1)}(D_k)$. For $\Gamma \ll a_0[2(N+1)/3]^{-1/2}$, we then find

$$A_{\mathrm{nl,bl}}(\omega) = -\frac{\pi\eta}{4\hbar^3\Gamma^2} \sum_{k=1}^{N} |\mu_{0k}|^4 P^{(1)}(\omega - \Omega_k^0), \qquad (26)$$

which is a series of Gaussian peaks centered at the homogeneous one-exciton frequencies, with widths σ_k and weights $|\mu_{0k}|^4$. The bleaching of the $k=1$ one-exciton transition will by far be the strongest feature in this part of the spectrum. It is clear from Eq. (26) that the bleaching features in the nonlinear absorption spectrum exhibit exactly the same motional narrowing effects as the linear absorption spectrum [Eq. (22)].

We now turn to the nonlinear absorption contribution derived from $\gamma^{(3)}_{\mathrm{TPA}}$. This part of the susceptibility describes two-photon absorption (TPA), with resonances whenever 2ω equals a two-exciton energy $\Omega_{k_3} + \Omega_{k_4}$. We focus on the resonance with the two-exciton $|k',k''\rangle$ and assume that its frequency $(\Omega_{k'}+\Omega_{k''})/2$ is well-separated from all one-exciton frequencies in the same aggregate. Here, "well-separated" means an energy difference that is large compared to Γ as well as large compared to the spread in the separation caused by static disorder, so that all frequencies in the nonresonant factors in Eq. (24c) can be replaced by their homogeneous values (we comment on this condition at the end of this section). Then, the nonlinear absorption in the vicinity of the two-photon resonance simplifies to

$$A_{\mathrm{nl,TPA}}(\omega) = \left\langle \frac{\eta\Gamma}{\hbar^3} \frac{|M_{0,k'k''}|^2}{[\omega - (\Omega^0_{k'}+\Omega^0_{k''})/2 - (D_{k'}+D_{k''})/2]^2 + \Gamma^2} \right\rangle, \qquad (27)$$

with the two-photon transition moment defined as

$$M_{0,k'k''} = \sum_{k=1}^{N} \frac{\mu_{0,k}\mu_{k,k'k''}}{\Omega^0_{k'}+\Omega^0_{k''}-2\Omega^0_k}. \qquad (28)$$

The disorder average in Eq. (27) now only involves the marginal distribution for $(D_{k'}+D_{k''})/2$, half the inhomogeneous offset of the two-exciton frequency. From Sec. IV, it is clear that this distribution is a Gaussian $G[(D_{k'}+D_{k''})/2]$, with vanishing mean and with variance $\sigma^2_{k'k''}/4 = (B_{k'k'} + B_{k''k''} + 2B_{k'k''})/4$ [cf. Eq. (17)]. In general, the disorder average of the TPA peak thus leads to a Voigt profile. If we restrict to the case $2\Gamma \ll \sigma_{k'k''}$, however, we obtain a Gaussian peak

$$A_{\mathrm{nl,TPA}}(\omega) = (\pi\eta/\hbar^3)\,|M_{0,k'k''}|^2 G[\omega - (\Omega^0_{k'}+\Omega^0_{k''})/2]. \qquad (29)$$

Using Eq. (12), we find that the width $\sigma_{k'k''}/2$ of the TPA peak related to the two-exciton $|k',k''\rangle$ varies between $a_0[4(N+1)/5]^{-1/2}$ for $\beta=0$ [if $k',k'' \neq (N+1)/2$] and a_0 for $\beta \to 1$. As in the case of linear absorption, we thus observe motional narrowing in the TPA spectrum, which decreases for increasing intersite correlation. It is noteworthy that if the exciton energies would be uncorrelated $P^{(2)}(D_{k'},D_{k''}) = P^{(1)}(D_{k'})P^{(1)}(D_{k''})$, the TPA peak would have a width of $a_0[4(N+1)/3]^{-1/2}$ ($\beta=0$); the actual width of the TPA peak is larger because of the positive correlations between $D_{k'}$ and $D_{k''}$. For β small, a similar approximation as in Eq. (21) leads to $[(1+\beta)/(1-\beta)]^{1/2}a_0[4(N+1)/5]^{-1/2}$ for the width of the TPA peak.

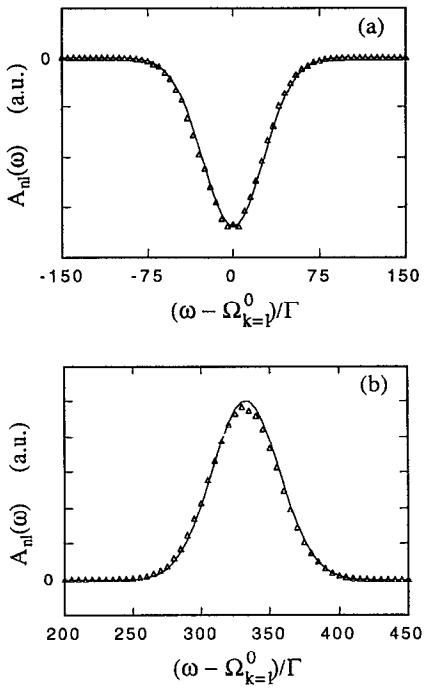

FIG. 3. (a) The $k=1$ one-exciton bleaching peak for an ensemble of J aggregates of $N=20$ molecules with $a_0=10^{-2}|V|$, $\beta=0$, and $\Gamma=10^{-4}|V|$. The solid line gives the motional narrowing result [Eq. (26)] and the markers indicate data points obtained from exact numerical simulations (see Ref. 16). (b) The two-photon absorption peak related to the $|k'=2,k''=1\rangle$ two-exciton state. Curves and parameters are the same as in (a). The motional narrowing result was obtained from Eq. (27). We note that for the parameters used here, the peak two-photon absorption is roughly five orders of magnitude smaller than the peak bleaching in (a).

The strongest TPA peak is the one related to the $|k'=2,k''=1\rangle$ two-exciton, which is predominantly reached through the one-exciton $|k=1\rangle$ as intermediate state [relevant oscillator strengths $\mu^2_{0,1} \approx 0.81(N+1)\mu^2$ and $\mu^2_{1,21} \approx 1.27(N+1)\mu^2$]. In Fig. 3, a comparison is made between the motional narrowing result and the exact forms of the $|k=1\rangle$ bleach and the $|k'=2,k''=1\rangle$ two-photon absorption features for J aggregates of 20 molecules with $a_0=10^{-2}|V|$, $\beta=0$, and $\Gamma=10^{-4}|V|$. The exact line shapes were obtained through numerical simulation along the method described in Ref. 16. Figure 3 demonstrates clearly the motional narrowing of the local disorder; without this effect, both the bleaching and the TPA peak would have a FWHM of roughly $2.35a_0=235\Gamma$. It is also clearly observed that for the small disorder value used here, the perturbative treatment of the motional narrowing limit is sufficient to accurately describe the line shapes.

We finally comment briefly on the condition imposed above Eq. (27) that the separation between the two-photon resonances and the one-exciton frequencies be large

compared to the spread in this separation caused by the static disorder. This condition is less restrictive than it seems. As an explicit example, consider the TPA peak related to the $|2,1\rangle$ two-exciton. The inhomogeneous component in the frequency separation to the $k=1$ one-exciton state, $(D_{k=2}-D_{k=1})/2$, has a Gaussian distribution with vanishing mean and width $0.5(B_{11}+B_{22}-2B_{12})^{1/2}$, which varies between $a_0[4(N+1)]^{-1/2}$ for $\beta=0$ and 0 for $\beta\to 1$. Thus, we see that in the case of small correlations, the condition of large relative separation is not very restrictive because of the motional narrowing and the positive correlations between $D_{k=1}$ and $D_{k=2}$. For strong intersite correlations, the condition is not restrictive because of the perfect correlations which then exist between all exciton frequencies on a single chain.

C. Two-color pump–probe spectroscopy

As a final example, we discuss two-color pump–probe spectroscopy. In this technique, the sample is first irradiated with a short pump pulse of frequency ω_1; a variable delay time τ later, the state of the sample is probed by a laser with frequency ω_2. The differential absorption spectrum $\Delta A(\omega_1,\omega_2;\tau)$ is defined as the difference between the probe absorption with and without pump pulse. To lowest order in the laser intensities, this spectrum measures third-order response functions.[35] A more intuitive view of the experiment, however, is to treat it as a sequence of two linear absorption experiments. First, linear absorption of the pump pulse creates one-excitons. During the delay time, the one-excitons can decay to the ground state or redistribute over the one-exciton band through scattering on phonons. Finally, the state of the system is probed by measuring the linear absorption of the probe pulse. As the probe absorption takes place in a prepared system, in which population has been taken away from the ground state to the one-exciton band, the differential absorption spectrum contains contributions arising from (i) stimulated emission from the one-exciton states; (ii) bleaching of the transitions from the ground state to the one-exciton band; and (iii) the excitation of two-excitons. This simplified picture of the experiment is justified if the delay is long compared to the pulse durations and the dephasing time of the coherences between and inside the exciton bands. If this is not the case, also contributions to the differential absorption exist in which, e.g., the two interactions with the pump pulse excite a coherence between the ground state and two-exciton states, which is observed by the interaction with the probe pulse.

In Appendix B, we derive the differential absorption spectrum within the above view for pulse durations that are short compared to the dephasing times. The general result (B9) is not restricted to the motional narrowing limit and holds for arbitrary dynamics within the space of one-exciton populations. Here, however, we restrict ourselves to discussing the motional narrowing limit and we will assume a simple exponential decay of the population of the kth one-exciton with rate γ_k. Then, Eq. (B9) reduces to

$$\Delta A(\omega_1,\omega_2;\tau)=-C\sum_{k_1,k_2=1}^{N}\exp(-\gamma_{k_1}\tau)\,|\mu_{0k_1}\mu_{0k_2}|^2(1+\delta_{k_1,k_2})\langle\hat{I}_1(\omega_1-\Omega^0_{k_1}-D_{k_1})\hat{I}_2(\omega_2-\Omega^0_{k_2}-D_{k_2})\rangle$$
$$+C\sum_{\substack{k_1,k_2,k_3=1\\ k_2>k_3}}^{N}\exp(-\gamma_{k_1}\tau)\,|\mu_{0k_1}\mu_{k_1,k_2k_3}|^2\langle\hat{I}_1(\omega_1-\Omega^0_{k_1}-D_{k_1})\hat{I}_2(\omega_2+\Omega^0_{k_1}+D_{k_1}-\Omega^0_{k_2}-D_{k_2}-\Omega^0_{k_3}-D_{k_3})\rangle. \tag{30}$$

Here, C is a constant and $\hat{I}_1(\omega)$ and $\hat{I}_2(\omega)$ denote the power spectra of the envelopes of the pump and the probe pulse, respectively. The first part of Eq. (30) contains the contributions from stimulated emission (the δ_{k_1,k_2} term) and bleaching (the "1" term), which result in a negative differential absorption; the second part describes the positive (induced) absorption of photons that cause the transition from the $|k_1\rangle$ one-exciton to the $|k_2,k_3\rangle$ two-exciton.

In general, the disorder averages in Eq. (30) involve the joint distribution for two of the one-exciton frequencies (the first term) and the joint distribution for a one-exciton and a two-exciton frequency (the second term). If we restrict ourselves to the strongest spectral features, however, we set $k_1=k_2=1$ in the first term and $k_1=k_3=1$, $k_2=2$ in the second term

$$\Delta A(\omega_1,\omega_2;\tau)=-2C\exp(-\gamma_1\tau)\,|\mu_{01}|^4\langle\hat{I}_1(\omega_1-\Omega^0_1-D_1)\times\hat{I}_2(\omega_2-\Omega^0_1-D_1)\rangle$$
$$+C\exp(-\gamma_1\tau)\,|\mu_{01}\mu_{1,21}|^2\times\langle\hat{I}_1(\omega_1-\Omega^0_1-D_1)\hat{I}_2(\omega_2-\Omega^0_2-D_2)\rangle. \tag{31}$$

Now, the first contribution (bleach and stimulated emission) only involves the distribution $P^{(1)}(D_1)$, whereas the second contribution (induced absorption) involves the joint distribution $P^{(2)}(D_1,D_2)$ [cf. Eqs. (16)].

For Gaussian power spectra, the averages in Eq. (31) lead to analytically solvable Gaussian integrals. The results are rather convoluted. Instead, much simpler and more transparent results can be obtained for general pulse shapes

in the limit where the spectral pulse width is small compared to the width of the exciton frequency distributions. For the first average, this condition implies that the pulse is narrow compared to the J band. Then

$$\langle \hat{I}_1(\bar{\omega}_1 - D_1)\hat{I}_2(\bar{\omega}_2 - D_1)\rangle$$
$$\approx P^{(1)}(\bar{\omega}_1)\int_{-\infty}^{+\infty} dD_1\, \hat{I}_1(\bar{\omega}_1 - D_1)\hat{I}_2(\bar{\omega}_2 - D_1)$$
$$= P^{(1)}(\bar{\omega}_1)(\hat{I}_1 * \hat{I}_2)(\omega_1 - \omega_2), \tag{32}$$

where $\bar{\omega}_j \equiv \omega_j - \Omega_1^0$ and $(\hat{I}_1 * \hat{I}_2)(\omega)$ denotes the convolution of the two power spectra evaluated at the frequency ω. In the last equality of Eq. (32), it has been assumed that at least one of the power spectra is symmetric. In the limit of small pulse widths, the second average leads to

$$\langle \hat{I}_1(\bar{\omega}_1 - D_1)\hat{I}_2(\bar{\omega}_2 - D_2)\rangle$$
$$\approx P^{(2)}(\bar{\omega}_1, \bar{\omega}_2)\int_{-\infty}^{+\infty} dD_1\, dD_2\, \hat{I}_1(\bar{\omega}_1 - D_1) \times \hat{I}_2(\bar{\omega}_2 - D_2)$$
$$= P^{(2)}(\bar{\omega}_1, \bar{\omega}_2)\hat{I}_1\hat{I}_2, \tag{33}$$

where $\bar{\omega}_2 \equiv \omega_2 - \Omega_2^0$, and $\hat{I}_j$ denotes the total (integrated) power of pulse j. We thus obtain for the pump–probe signal

$$\Delta A(\omega_1, \omega_2; \tau) = -2C \exp(-\gamma_1 \tau)\,|\mu_{01}|^4 P^{(1)}(\omega_1 - \Omega_1^0) \times \left[(\hat{I}_1 * \hat{I}_2)(\omega_1 - \omega_2) - \frac{|\mu_{1,21}|^2}{2|\mu_{0,1}|^2} \times P^{(c)}(\omega_2 - \Omega_2^0 | \omega_1 - \Omega_1^0)\hat{I}_1\hat{I}_2 \right]. \tag{34}$$

Here, $P^{(c)}(D_2 | D_1) \equiv P^{(2)}(D_1, D_2)/P^{(1)}(D_1)$ denotes the conditional probability[24] for the inhomogeneous frequency offset of the $|k=2\rangle$ one-exciton, given the frequency offset of the $|k=1\rangle$ one-exciton. The result (34) has a simple interpretation—the overall *magnitude* of the pump–probe signal is determined by the absorption of the pump pulse, which is proportional to $P^{(1)}(\omega_1 - \Omega_1^0)$ (the J band) and the exponential decay during the pump–probe delay. The *shape* of the pump–probe signal is determined by the factor in square brackets in Eq. (34). For narrow pulses, a bleach (and stimulated emission) will be observed at frequency ω_2 only if the pump and probe pulses overlap, which explains the convolution. Induced absorption is observed at ω_2 only if the probe pulse is resonant with the transition from the $|k=1\rangle$ one-exciton to the $|k_1=2, k_2=1\rangle$ two-exciton in aggregates that have their $|k=1\rangle$ one-exciton frequency resonant with the pump pulse. This explains the conditional probability.

The general conditional probability for the frequency offset $D_{k'}$, given the value of D_k, is easily calculated from Eqs. (16). We obtain the Gaussian

$$P^{(c)}(D_{k'} | D_k) = \frac{1}{\sqrt{2\pi\sigma^c_{kk'}}} \exp\left[-\left(D_{k'} - \frac{B_{kk'}}{B_{kk}} D_k \right)^2 \Big/ 2(\sigma^{c2}_{kk'}) \right], \tag{35a}$$

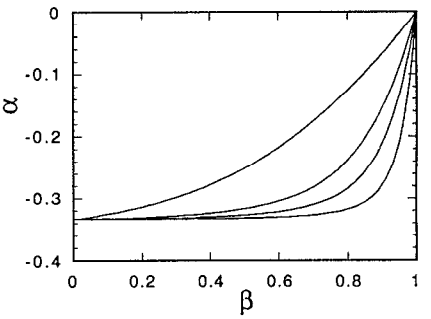

FIG. 4. The slope α defined in Eq. (36) as a function of the degree of intersite correlation β. From top to bottom, the curves apply to aggregates of $N=10$, 30, 50, and 100 molecules, respectively.

with the standard deviation

$$\sigma^c_{kk'} = (B_{k'k'} - B^2_{kk'}/B_{kk})^{1/2} \tag{35b}$$

and $B_{kk'}$ as defined in Eqs. (11) and (12). It should be noted that, in general, the mean of the conditional probability $(B_{kk'}/B_{kk})D_k$ does not vanish, as the covariance $B_{kk'}$ is not equal to zero. For $1-\beta \gg \beta[2\pi k^{(\prime)}/(N+1)]^2$ (and in particular for $\beta=0$), the mean value is found to be $(2/3)D_k$ [if $k' \neq (N+1)/2$ *and* $k+k' \neq (N+1)/2$] and the width $\sigma^c_{kk'} = a_0[(1+\beta)/(1-\beta)]^{1/2}[6(N+1)/5]^{-1/2}$, which is then roughly equal to the width of the J band [Eq. (21)]. In the limit of strong correlations ($\beta \to 1$), the average of the conditional probability approaches D_k and the width vanishes.

We will now apply the above knowledge of the conditional probability to discuss the differential absorption spectrum. The maximum of the bleach occurs (for symmetric pulse shapes) at $\omega_2 = \omega_1$, while the maximum of the induced absorption occurs at the mean value of $P^{(c)}(\omega_2 - \Omega_2^0 | \omega_1 - \Omega_1^0)$, i.e., at $\omega_2 - \Omega_2^0 = (\omega_1 - \Omega_1^0)B_{12}/B_{11}$. Thus, the frequency separation between the absorption and bleach peaks is given by[36]

$$\Delta_{\text{abs,bl}} = \alpha(\omega_1 - \Omega_1^0) + (\Omega_2^0 - \Omega_1^0) \tag{36a}$$

with

$$\alpha \equiv B_{12}/B_{11} - 1. \tag{36b}$$

Using Eq. (12), we find that the factor α varies between $-1/3$ ($\beta=0$) and $0(\beta \to 1)$. The full β dependence of α has been plotted in Fig. 4 for various aggregate sizes. The interesting point is that α does not depend on a_0. Thus, assuming that N is known, the *separation* between the induced absorption and the bleach as a function of the detuning of the pump frequency from the J-band maximum, $\omega_1 - \Omega_1^0$, gives direct information on β alone. By contrast, the *width* σ^c_{12} of the induced-absorption peak depends on both β and a_0, but not on the pump frequency. The dependence on a_0 is a simple proportionality; the β dependence is, for several values of N, given in Fig. 5. If β is known from measuring α, the width of the induced-absorption peak can thus be used to obtain a_0.

The important conclusion is that, in contrast to linear absorption measurements, *two-color pump–probe experi-*

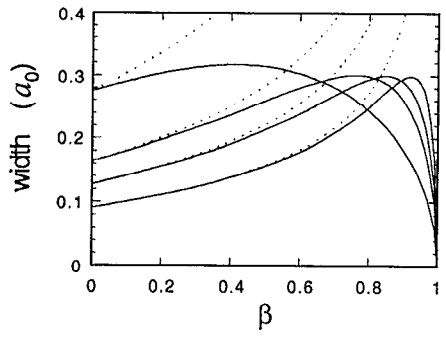

FIG. 5. Width σ_{12}^c of the conditional probability for the value of the $k=2$ one-exciton frequency, given the $k=1$ one-exciton frequency, as a function of the degree of intersite correlation β for several aggregate sizes. The solid curves give the exact results [Eq. (35b)] and the dotted curves represent the small-β approximation $a_0[(1+\beta)/(1-\beta)]^{1/2}[6(N+1)/5]^{-1/2}$. From top to bottom (at $\beta=0$), the curves correspond to $N=10$, 30, 50, and 100, respectively. If σ_{12}^c is large compared to the width of the convolution of the pump and probe power spectra, it directly gives the width of the induced-absorption peak in the differential absorption spectrum.

ments can be used to obtain separate information on both the correlation and the magnitude of the microscopic disorder. We also note that the constant term $\Omega_2^0-\Omega_1^0$ in Eq. (36a) gives information on the interaction and the size N of the aggregate [Eq. (6b)].

One aspect of the above should be treated with more caution—the limited validity of Eq. (33) in the case of strong correlations ($\beta\to 1$), where the joint distribution function $P^{(2)}(D_1,D_2)$ approaches the form $P^{(1)}(D_1)\delta(D_2-D_1)$. Evidently, $P^{(2)}(D_1,D_2)$ will then not be broad compared to the laser pulses in all directions of the (D_1,D_2) space, no matter how narrow the laser pulses are, and the first step in Eq. (33) is invalid. In fact, the criterion for applicability of Eq. (33) is that σ_{12}^c is large compared to the width of $(\hat{I}_1*\hat{I}_2)(\omega)$; in the limit $\beta\to 1$, this cannot be satisfied as σ_{12}^c vanishes (Fig. 5). To obtain an improved theory in this limit, we may use the $\delta(D_2-D_1)$ nature of the distribution and eliminate the D_2 integration in Eq. (33). In analogy to Eq. (32), we then obtain

$$\langle \hat{I}_1(\bar{\omega}_1-D_1)\hat{I}_2(\bar{\omega}_2-D_1)\rangle \approx P^{(1)}(\omega_1-\Omega_1^0)(\hat{I}_1*\hat{I}_2)(\omega_1-\omega_2-\Omega_1^0+\Omega_2^0). \quad (37)$$

From this, we see that in the presence of strong correlations, the frequency separation between the induced absorption and the bleach peak is given by $\Omega_2^0-\Omega_1^0$, irrespective of the pump freqency, which is the same result as obtained from Eq. (36) in the limit $\beta\to 1$. Thus, the conclusion that measurement of $\Delta_{\mathrm{abs,bl}}$ as a function of $\omega_1-\Omega_1^0$ allows for the determination of β stays valid. We also observe from Eq. (37) that for strong correlations, the width of the induced-absorption peak is determined by the convolution of the power spectra of the pump and probe beams and does not vanish. Therefore, if β is found to be close to unity, caution must be used when applying Fig. 5 to obtain a_0. Then, one either has to account for the finite width of $(\hat{I}_1*\hat{I}_2)(\omega)$ by deconvolution, or one may resort to using the width of the J band (Fig. 2) to obtain a_0.

VI. DISCUSSION AND CONCLUDING REMARKS

It is by now well-established that static disorder plays a key role in the optical properties of molecular aggregates.[7,14,37–39] In this paper, we have studied nonlinear optical line shapes of disordered linear molecular aggregates within the motional narrowing limit. Our model assumes Gaussian diagonal disorder with arbitrary intersite correlations. The theory presented is general and not limited to first- and third-order optical response. This is a consequence of two important features combined in our model. (i) The energies of all multiexciton states of the linear chain with nearest-neighbor interactions can be expressed as sums of one-exciton energies.[15,27,28] (ii) As shown in Sec. IV [Eqs. (15) and (12)], to first order in the disorder the complete joint stochastic distribution function for the one-exciton energies of an aggregate can be obtained exactly, irrespective of the magnitude of the intersite correlations. In general, linear optical techniques are only sensitive to the marginal distributions for the one-exciton frequencies [$P^{(1)}$], while third-order techniques involve distributions for two one-exciton frequencies and one two-exciton frequency (derived from $P^{(4)}$). Higher-order techniques involve yet higher-order marginal distributions.

The motional narrowing limit is a lowest-order expansion in the disorder: The exciton wave functions are taken identical to those of the homogeneous aggregate and their energies are taken to first order in the disorder.[4,29] Strictly speaking, this limits the approach to small disorder values and (or) small chain lengths. The criterion for applicability is easily derived by requiring that the energy separation between any pair of one-exciton states on the homogeneous chain is large compared to the disorder induced width of this separation.[4] For vanishing intersite correlation ($\beta=0$), this leads directly to $a_0N^{3/2}/\pi^2|V|\ll 1$. In fact, this criterion expresses the strongest limitation, as the approach improves for increasing correlation β and eventually becomes exact for all chain lengths and disorder values in the limiting case of infinitely strong intersite correlations ($\beta=1$), where each individual aggregate is homogeneous.

In practice, the size of molecular aggregates is often too large to meet the above criterion for a perturbative treatment and the disorder localizes the exciton states on parts of the aggregate.[38,40,41] Nevertheless, the motional narrowing limit can still be useful, provided that we replace in all expressions contained in this paper the real chain length by the typical delocalization length N_{del} of the exciton states in the energy region of interest (usually the band edge). This procedure has already been suggested by Knapp[4] and its power has been demonstrated before. For instance, numerically obtained scaling laws for the nonlinear response of disordered aggregates could be reproduced using this approach.[14] Furthermore, we note that the measured two-color pump–probe spectrum of aggregates of pseudo-isocyanine can be reproduced surprisingly well[7] by using the simple motional narrowing expressions worked

out in Sec. V C in combination with the delocalization length and disorder value that were previously found from linear optical experiments.[38] An effect that cannot be covered by the above procedure is that the line shapes usually become asymmetric at higher disorder values (the J band then obtains a Lorentzian high-energy side).[38,42]

One of the key points of the present paper is the role of intersite correlations in the disorder of the molecules on a chain. As the disorder is usually induced by a random environment (such as a glassy host), it is very likely that such correlations exist for neighboring molecules. If correlations are included, there are four parameters that affect the optical line shapes—the intermolecular interaction (V), the size of the aggregates (N or rather $N_{\rm del}$), the local disorder (a_0), and the degree of correlation (β). The interaction can be estimated from the shift $2V$ of the J band relative to the monomer transition. Furthermore, $N_{\rm del}$ may be obtained from the superradiant fluorescence decay.[5,33,34] This leaves two unknown parameters to be determined from optical line shapes. As has been argued in Sec. V A, the linear absorption spectrum does not yield independent information on a_0 and β, and is therefore not an ideal tool to get insight into the microscopic disorder model. By contrast, we have shown in Sec. V C that two-color pump–probe experiments do yield extra information. In particular, measuring the energy separation ($\Delta_{\rm abs,bl}$) between the bleach and induced-absorption peaks as a function of the detuning of the pump frequency relative to the J-band center yields the slope α in Eq. (36), which is insensitive to the local disorder and is (for fixed chain length) a function of the degree of correlation only (Fig. 4). Having obtained β, one may then use the width of the induced-absorption peak (Fig. 5) or the width of the J band (Fig. 2) to estimate a_0. In principle, it is even possible to independently obtain N ($N_{\rm del}$) from the pump–probe experiment, namely from the value of $\Delta_{\rm abs,bl}$ when the pump is tuned to the J-band center. We finally note that the width of the induced-absorption peak yields alternative information on correlations. For low degree of correlation, this width is of the same order as the width of the J band, whereas for very strong correlations, the induced absorption is generally much narrower than the J band and is limited by the laser linewidths only.

Even though the theory for two-color pump–probe experiments presented here is approximate, result (34) contains the basic physics and clearly suggests a novel way to experimentally obtain detailed information on the character of the energetic disorder in aggregates. This in turn may lead to information on the structural disorder in the host medium (glass or solution). Equation (34) has already been used successfully to analyze pump–probe experiments on aggregates of pseudo-isocyanine.[7] The theory may be improved in a straightforward way by determining the averages in Eqs. (32) and (33) exactly, which is possible for Gaussian line shapes. Also, no major complications are encountered when keeping more exciton levels than $|k=1\rangle$ and $|k_1=2, k_2=1\rangle$ in working out Eq. (30). Further improvement is only possible by relaxing the perturbative treatment of the disorder and numerically simulating the differential absorption spectrum [Eq. (B9)]. Preliminary results of such calculations indicate that also outside the perturbative regime, the pump–probe experiment provides a useful tool to characterize the microscopic disorder.[44]

ACKNOWLEDGMENTS

It is a pleasure to thank James Durrant for stimulating discussions. Financial support by the Netherlands Organization for Scientific Research (NWO) through the award of a Huygens Fellowship is gratefully acknowledged.

APPENDIX A: THE COVARIANCE MATRIX FOR THE EXCITON FREQUENCIES

In this appendix, we derive Eq. (12) for the covariance matrix $B_{kk'}\equiv\langle D_k D_{k'}\rangle$ of the exciton frequencies to first order in the diagonal disorder. We start from Eq. (11), which after substitution of Eqs. (3) and (6a), yields

$$B_{kk'}=\left(\frac{a_0}{N+1}\right)^2\sum_{n,m=1}^{N}(1-\cos pn)(1-\cos p'm)\times\exp(-|n-m|/l_0), \tag{A1}$$

where $p=2\pi k/(N+1)$ and $p'=2\pi k'/(N+1)$. From this, we obtain

$$B_{kk'}=\left(\frac{a_0}{N+1}\right)^2[F(p,p')+G(p,p')+G(p',p)] \tag{A2}$$

with

$$F(p,p')=\sum_{n=1}^{N}(1-\cos pn)(1-\cos p'n) \tag{A3}$$

and

$$G(p,p')=\sum_{m=1}^{N}\sum_{n=1}^{m-1}(1-\cos pn)(1-\cos p'm)\times\exp[(n-m)/l_0]. \tag{A4}$$

The single summation in Eq. (A3) is easily decomposed in standard summations [Eq. (1.342) of Ref. 43], which leads to

$$F(p,p')=(N+1)[1+(\delta_{k,k'}+\delta_{k+k',N+1})/2]. \tag{A5}$$

Also the n summation and the subsequent m summation in Eq. (A4) only involve standard expressions [Eqs. (1.342) and (1.353) of Ref. 43], application of which leads to

$$G(p,p')=\frac{\beta}{1-\beta}(N+1)+\frac{1}{2}\beta(N+1)\frac{\cos p-\beta}{1-2\beta\cos p+\beta^2}\times(\delta_{k,k'}+\delta_{k+k',N+1})-(1-\beta^{N+1})f(p)f(p') \tag{A6}$$

with

$$f(p)=\frac{1}{1-\beta}-\frac{1-\beta\cos p}{1-2\beta\cos p+\beta^2}. \tag{A7}$$

In deriving the above forms for $F(p,p')$ and $G(p,p')$, we used the fact that $\sin[(N+1)p/2]=0$, $\cos(N+1)p=1$, and $\cos(Np)=\cos p$ for $p=2\pi k/(N+1)$ with k integer. Combining Eqs. (A2), (A5), and (A6), we obtain Eq. (12) of the main text.

APPENDIX B: DERIVATION OF THE PUMP–PROBE SIGNAL

In this appendix, we derive the differential absorption for a two-color pump–probe experiment on molecular aggregates. We restrict ourselves to the intuitive picture discussed in the main text, where the experiment is considered a succession of two linear absorption experiments. We will give a general derivation, which is not limited to the motional narrowing limit, i.e., the labels k used below do not necessarily refer to the homogeneous states.

Let the electric fields of the pump and probe pulses be given by

$$E_1(t)=\hat{E}_1(t)\exp(-i\omega_1 t)+\text{c.c.} \tag{B1a}$$

and

$$E_2(t)=\hat{E}_2(t-\tau)\exp(-i\omega_2 t)+\text{c.c.}, \tag{B1b}$$

respectively. Here, ω_1 and ω_2 are the central frequencies of the pulses and $\hat{E}_j(t)$ are slowly varying envelopes, centered around $t=0$. The power spectra of the envelopes are then given by

$$\hat{I}_j(\omega)=\frac{1}{2\pi}\left|\int_{-\infty}^{\infty} dt\,\hat{E}_j(t)\exp(-i\omega t)\right|^2. \tag{B2}$$

$\hat{I}_j(\omega)$ is centered around $\omega=0$ and its width is the inverse pulse duration.

The contribution of a single aggregate to the linear absorption of a laser pulse with frequency ω is governed by its linear polarizability[26]

$$\gamma^{(1)}(-\omega;\omega)=\frac{1}{\hbar}\sum_{a,b}p_a(0)\left(\frac{|\mu_{ab}|^2}{\Omega_b-\Omega_a-\omega-i\Gamma_{ab}}+\frac{|\mu_{ab}|^2}{\Omega_b-\Omega_a+\omega+i\Gamma_{ab}}\right), \tag{B3}$$

where μ_{ab} is the transition dipole between the levels a (frequency Ω_a) and b (frequency Ω_b) of the aggregate and Γ_{ab} denotes the homogeneous dephasing rate of this transition. The summations over a and b run over all levels, i.e., the ground state, one-excitons, two-excitons, etc. Finally, $p_a(0)$ denotes the population of level a before the interaction with the pulse. If the aggregate is initially in its ground state and we invoke the RWA, Eq. (B3) reduces to Eq. (20). To first order in the power spectrum, the absorbed power of pulse j is now given by

$$A_j\propto\int_{-\infty}^{+\infty} d\omega_j'\hat{I}_j(\omega_j-\omega_j')\,\mathrm{Im}\,\gamma^{(1)}(-\omega_j';\omega_j'), \tag{B4}$$

where the integration over ω_j' must be included to account for pulses that are short compared to the homogeneous dephasing times $1/\Gamma_{ab}$.

Before the pump pulse arrives, the aggregate is in the ground state, i.e., $p_a(0)=1$ if a is the ground state and $p_a(0)=0$ otherwise. Application of Eqs. (B3) and (B4) to this situation shows that, to first order in the intensity, the pump pulse excites one-exciton populations, which are, within the RWA, given by

$$p_k(0^+)\propto\int_{-\infty}^{\infty} d\omega_1'\,\hat{I}_1(\omega_1-\omega_1')\frac{|\mu_{0k}|^2\Gamma}{(\omega_1'-\Omega_k)^2+\Gamma^2}. \tag{B5}$$

Here, we assumed that all transitions between the ground state and the one-exciton band have the same dephasing rate. During the delay period, which is assumed long compared to the laser pulses and the dephasing times, the one-exciton populations can decay to the ground state or redistribute over the one-exciton band by scattering on other elementary excitations. We will not model this dynamics, but instead formulate our result in terms of a general Green's function $G_{kk'}(t)$ describing the evolution of the one-exciton populations during the delay. We will assume that this Green's function varies slowly compared to the pulse durations. Then, we can write for the populations just before the probe pulse arrives

$$p_k(\tau^-)=\sum_{k'=1}^{N}G_{kk'}(\tau)p_{k'}(0^+), \tag{B6a}$$

$$p_g(\tau^-)=1-\sum_{k,k'=1}^{N}G_{kk'}(\tau)p_{k'}(0^+), \tag{B6b}$$

where p_g is the ground state population. We now apply Eqs. (B3) and (B4) to calculate the linear absorption of the probe pulse in the system with populations given by Eq. (B6). This gives rise to four types of contributions. (i) The probe pulse can cause stimulated emission of the one-excitons $|k\rangle$. (ii) The probe pulse can be absorbed by inducing a transition from the excited one-excitons to the two-exciton band. (iii) The first term in Eq. (B6b) is the equilibrium population; in the differential absorption, this is exactly canceled by the absorption of the probe pulse without pumping. (iv) The second term in Eq. (B6b) is the loss of population in the ground state and will give rise to a bleach of all transitions from the ground state to the one-exciton band. Contributions (i) and (iv) to the differential absorption are negative, whereas contribution (ii) is positive. Using Eqs. (B3)–(B6) and adding the disorder average, we obtain for the differential absorption in the RWA

$$\Delta A(\omega_1,\omega_2;\tau)=-\frac{C}{\pi^2}\left\langle \int_{-\infty}^{\infty} d\omega_1' \int_{-\infty}^{\infty} d\omega_2' \hat{I}_1(\omega_1-\omega_1')\hat{I}_2(\omega_2-\omega_2') \sum_{k_1=1}^{N} \frac{|\mu_{0k_1}|^2\Gamma}{(\omega_1'-\Omega_{k_1})^2+\Gamma^2} \left\{ \sum_{k_2=1}^{N} \left[\sum_{k_3=1}^{N} G_{k_3k_1}(\tau) + G_{k_2k_1}(\tau) \right] \frac{|\mu_{0k_2}|^2\Gamma}{(\omega_2'-\Omega_{k_2})^2+\Gamma^2} - \sum_{\substack{k_2,k_3,k_4=1 \\ k_3>k_4}}^{N} G_{k_2k_1}(\tau) \frac{|\mu_{k_2,k_3k_4}|^2\Gamma'}{(\omega_2'+\Omega_{k_2}-\Omega_{k_3}-\Omega_{k_4})^2+\Gamma'^2} \right\} \right\rangle . \tag{B7}$$

Here, Γ' is the homogeneous dephasing rate of the transitions between the one- and the two-exciton bands and C is a constant that contains, among other things, the density of aggregates (π^2 has been added for future convenience). The three terms within curly brackets in Eq. (B7) are, respectively, the bleach, the stimulated emission, and the absorption to two-exciton states. A full-blown expansion of the density matrix to third order in the pulse amplitudes[35] gives the same result as Eq. (B7), provided the delay time τ is long compared to the decay times of coherences between and inside exciton bands, and the pulse durations are short compared to the dynamic time scale within the space of one-exciton populations.

We now restrict ourselves to the case that the pulse durations are short compared to the dephasing times ($1/\Gamma$ and $1/\Gamma'$), so that the power spectra are broad compared to the homogeneous exciton line shapes. We then have

$$\int_{-\infty}^{+\infty} d\omega_j' \frac{\hat{I}_j(\omega_j-\omega_j')\Gamma}{(\omega_j'-\Omega)^2+\Gamma^2}=\pi\hat{I}_j(\omega_j-\Omega) \tag{B8}$$

(analogously for $\Gamma\rightarrow\Gamma'$), so that Eq. (B7) reduces to

$$\Delta A(\omega_1,\omega_2;\tau)=-C\left\langle \sum_{k_1,k_2=1}^{N} \left\{ \sum_{k_3=1}^{N} G_{k_3k_1}(\tau)+G_{k_2k_1}(\tau) \right\} |\mu_{0k_1}\mu_{0k_2}|^2 \hat{I}_1(\omega_1-\Omega_{k_1})\hat{I}_2(\omega_2-\Omega_{k_2}) \right\rangle$$
$$+C\left\langle \sum_{\substack{k_1,k_2,k_3,k_4=1 \\ k_3>k_4}}^{N} G_{k_2k_1}(\tau) |\mu_{0k_1}\mu_{k_2,k_3k_4}|^2 \hat{I}_1(\omega_1-\Omega_{k_1})\hat{I}_2(\omega_2+\Omega_{k_2}-\Omega_{k_3}-\Omega_{k_4}) \right\rangle . \tag{B9}$$

We stress that this result is not restricted to the motional narrowing limit. That limit is obtained by using the transition dipoles of the homogeneous (multi)exciton states and replacing Ω_k by $\Omega_k^0+D_k$. If we furthermore assume that the one-exciton populations undergo no dynamics except for an exponential decay to the ground state with rate γ_k, we have $G_{kk'}(\tau)=\exp(-\gamma_k\tau)\delta_{kk'}$ and we obtain Eq. (30) of the main text.

[1] G. Scheibe, Angew. Chem. **50**, 212 (1937); E. E. Jelley, Nature **139**, 631 (1937).
[2] F. C. Spano and J. Knoester, in *Advances in Magnetic and Optical Resonance*, edited by W. S. Warren (Academic, New York, to be published), and references therein.
[3] A. Abragam, *Principles of Nuclear Magnetism* (Clarendon, Oxford, 1961).
[4] E. W. Knapp, Chem. Phys. **85**, 73 (1984).
[5] (a) S. de Boer, K. J. Vink, and D. A. Wiersma, Chem. Phys. Lett. **137**, 99 (1987); (b) S. de Boer and D. A. Wiersma, *ibid.* **165**, 45 (1990); (c) H. Fidder, J. Knoester, and D. A. Wiersma, *ibid.* **171**, 529 (1990).
[6] R. Hirschmann and J. Friedrich, J. Chem. Phys. **91**, 7988 (1989).
[7] H. Fidder, J. Knoester, and D. A. Wiersma, J. Chem. Phys. **98**, 6564 (1993).
[8] K. Minoshima, M. Taiji, and T. Kobayashi, in *1993 OSA Technical Digest Series* (Optical Society of America, Washington, D.C., 1993), Vol. 3, pp. 245–246.
[9] Y. Wang, Chem. Phys. Lett. **126**, 209 (1986); J. Opt. Soc. Am. B **8**, 981 (1991).
[10] V. L. Bogdanov, E. N. Viktorova, S. V. Kulya, and A. S. Spiro, Pis'ma Zh. Eksp. Teor. Fiz. **53**, 100 (1990) [JETP Lett. **53**, 105 (1991)].
[11] E. Hanamura, Phys. Rev. B **37**, 1273 (1988); **38**, 1228 (1988).
[12] (a) F. C. Spano and S. Mukamel, Phys. Rev. A **40**, 5783 (1989); (b) J. Chem Phys. **95**, 7526 (1991).
[13] H. Isihara and K. Cho, Phys. Rev. B **42**, 1724 (1990).
[14] J. Knoester, Chem. Phys. Lett. **203**, 371 (1993).
[15] F. C. Spano, Phys. Rev. Lett. **67**, 3424 (1991); **68**, 2976 (1992).
[16] J. Knoester, Phys. Rev. A **47**, 2083 (1993).
[17] A. Tilgner, H. P. Trommsdorff, J. M. Zeigler, and R. M. Hochstrasser, J. Chem. Phys. **96**, 781 (1992).
[18] Segment models are usually supplemented with a distribution of aggregate sizes.
[19] W. S. Warren and A. H. Zewail, J. Chem. Phys. **78**, 2298 (1983).
[20] L. Root and J. L. Skinner, J. Chem. Phys. **81**, 5310 (1984).
[21] L. Root and J. L. Skinner, Phys. Rev. B **32**, 4111 (1985).
[22] A. S. Davydov, *Theory of Molecular Excitons* (Plenum, New York, 1971).
[23] V. M. Agranovich and M. D. Galanin, in *Electronic Excitation Energy Transfer in Condensed Matter*, edited by V. M. Agranovich and A. A. Maradudin (North–Holland, Amsterdam, 1982).
[24] N. G. van Kampen, *Stochastic Processes in Physics and Chemistry* (North–Holland, Amsterdam, 1981).
[25] N. Bloembergen, *Nonlinear Optics* (Benjamin, New York, 1965).
[26] Y. R. Shen, *The Principles of Nonlinear Optics* (Wiley, New York, 1984).
[27] P. Jordan and E. Wigner, Z. Phys. **47**, 631 (1928).
[28] E. Lieb, T. Schultz, and D. Mattis, Ann. Phys. (N.Y.) **16**, 407 (1961).
[29] F. C. Spano, J. Phys. Chem. **96**, 2843 (1992).
[30] D. C. Mattis, *The Theory of Magnetism I* (Springer, Berlin, 1981), Chap. 5.9.
[31] See, e.g., H. Port, H. Nissler, and R. Silbey, J. Chem. Phys. **87**, 1994 (1987).
[32] R. Loudon, *The Quantum Theory of Light* (Clarendon, Oxford, 1983).
[33] M. Kasha, in *Spectroscopy of the Excited State*, edited by B. di Bartolo (Plenum, New York, 1976), Vol. 12.
[34] A. A. Muenter, D. V. Brumbaugh, J. Apolito, L. A. Horn, F. C. Spano, and S. Mukamel, J. Phys. Chem. **96**, 2783 (1992).
[35] Y. J. Yan, L. E. Fried, and S. Mukamel, J. Phys. Chem. **93**, 8149 (1989).
[36] In practice, overlap of the opposite bleach and induced-absorption peaks may lead to a larger effective separation of their maxima in the observed spectrum. When applying Eq. (36), this effect should be corrected for by decomposing the spectrum into separate bleach and absorption features.

[37] F. C. Spano and S. Mukamel, J. Chem. Phys. **91**, 683 (1989).
[38] H. Fidder, J. Knoester, and D. A. Wiersma, J. Chem. Phys. **95**, 7880 (1991).
[39] V. A. Malyshev, Opt. Spectrosc. **71**, 505 (1991).
[40] P. W. Anderson, Phys. Rev. **109**, 1492 (1958).
[41] D. J. Thouless, Phys. Rep. **13**, 93 (1974).
[42] M. Schreiber and Y. Toyozawa, J. Phys. Soc. Jpn. **51**, 1528 (1982).
[43] I. S. Gradshteyn and I. M. Ryzhik, *Table of Intergrals, Series, and Products* (Academic, New York, 1980).
[44] J. Durrant, J. Knoester, and D. A. Wiersma (in preparation).